Journal of the Formosan Medical Association (2012) 111, 471—481

Available online at www.sciencedirect.com

SciVerse ScienceDirect

journal homepage: www.jfma-online.com

ORIGINAL ARTICLE

Tension-compression viscoelastic behaviors of the periodontal ligament

Chen-Ying Wang [a,b], Ming-Zen Su [a,b], Hao-Hueng Chang [a,b], Yu-Chih Chiang [a,b], Shao-Huan Tao [c], Jung-Ho Cheng [c], Lih-Jyh Fuh [d,*], Chun-Pin Lin [a,b,**]

[a] *Graduate Institute of Clinical Dentistry, School of Dentistry, National Taiwan University, Taipei, Taiwan, ROC*
[b] *Department of Dentistry, National Taiwan University Hospital, Taipei, Taiwan, ROC*
[c] *Department of Mechanical Engineering, National Taiwan University, Taipei, Taiwan, ROC*
[d] *School of Dentistry & Graduate Institute of Dental Sciences, China Medical University, Taichung, Taiwan, ROC*

Received 1 April 2011; received in revised form 20 June 2011; accepted 27 June 2011

KEYWORDS
creep source;
finite element analysis;
periodontal ligament;
viscoelastic behavior

Background/Purpose: Although exhaustively studied, the mechanism responsible for tooth support and the mechanical properties of the periodontal ligament (PDL) remain a subject of considerable controversy. In the past, various experimental techniques and theoretical analyses have been employed to tackle this intricate problem. The aim of this study was to investigate the viscoelastic behaviors of the PDL using three-dimensional finite element analysis.

Methods: Three dentoalveolar complex models were established to simulate the tissue behaviors of the PDL: (1) deviatoric viscoelastic model; (2) volumetric viscoelastic model; and (3) tension-compression volumetric viscoelastic model. These modified models took into consideration the presence of tension and compression along the PDL during both loading and unloading. The inverse parameter identification process was developed to determine the mechanical properties of the PDL from the results of previously reported *in vitro* and *in vivo* experiments.

Results: The results suggest that the tension-compression volumetric viscoelastic model is a good approximation of normal PDL behavior during the loading-unloading process, and the deviatoric viscoelastic model is a good representation of how a damaged PDL behaves under loading conditions. Moreover, fluid appears to be the main creep source in the PDL.

* Corresponding author. DDS, School of Dentistry & Graduate Institute of Dental Sciences, China Medical University, Number 91, Hsueh-Shih Road, Taichung, Taiwan 40402, R.O.C.
** Corresponding author. School of Dentistry and Graduate Institute of Clinical Dentistry, National Taiwan University and National Taiwan University Hospital, Number 1, Chang Te Street, Taipei 10016, Taiwan, ROC.
E-mail addresses: ljfuh@mail.cmu.edu.tw (L.-J. Fuh), pinlin@ntu.edu.tw (C.-P. Lin).

doi:10.1016/j.jfma.2011.06.009

Conclusion: We believe that the biomechanical properties of the PDL established via retrograde calculation in this study can lead to the construction of more accurate extra-oral models and a comprehensive understanding of the biomechanical behavior of the PDL.

Introduction

The periodontal ligament (PDL) is a dense, fibrous, connective tissue that surrounds the root of the tooth and attaches the tooth to the alveolus in order to provide tooth support.[1] Like soft fibrous connective tissue elsewhere in the body, the PDL also consists of a fibrous stroma in a gel of ground substance that contains cells, blood vessels, and nerves. The fibrous stroma is composed primarily of collagen, while the cells are mainly fibroblasts.

Because the PDL is generally considered to be a suspensory ligament, several ideas such as tensile, compression, fluid-filled, and viscoelastic theories, have evolved to explain the intricacies of tooth support.[2–4] However, all of the current theories consider this to be a multiphase system that consists of fibers, ground substance, blood vessels, and fluid that interacts to resist mechanical forces. The results of past studies suggest that the viscoelastic theory best depicts the mechanisms within the PDL. After comparing PDL behavior with that of various types of mechanical springs and dampers, Bien arrived at the conclusion that the PDL behaves as a viscoelastic gel.[5] Moreover, Picton and Will listed five characteristics of a stressed periodontal ligament, all of which imply that the PDL possesses viscoelastic properties.[6]

Although many experimental techniques and theoretical analyses have been employed in the past to aid in the understanding the PDL, experiments concerning the PDL are especially difficult to perform due to its complex structure. With the hope of creating a more accurate representation of the PDL, we incorporated mathematical models into our data analysis. Mathematical modeling has been widely used and accepted as a supplementary research tool. Although not an exact representation of the human body, mathematical modeling has successfully answered questions regarding orthopedics, sports medicine, and the specifics of human movement. Numerous researchers have also become proponents of mathematical modeling because of its precision, credibility, and accurate results. Ross et al asserted that man can never know all the parts and transformations of a real system, but he may hope to establish a model that mimics it; e.g., when simulating a dynamical system, the model should satisfactorily mimic observed real-time behavior.[7] Yoshida et al took *in vivo* measurements of the elastic modulus of the human PDL and used the finite element method to simulate orthodontic tooth movement.[8] In addition, Walker et al gathered a great deal of perplexing experimental data and suggested that mathematical modeling might be able to clarify many of the unresolved questions regarding the PDL.[9] Clearly, mathematical modeling has steadily gained its share of advocates in dental research.

Finite element analysis is a specific type of mathematical modeling that has become the favored choice in theoretical biomechanical applications. It has been successfully applied to numerous biomechanical problems since its debut in the orthopedic biomechanics literature in 1972.[10] Although several finite element models of teeth (both with and without dental restorations) have been published, some models are two-dimensional[11,12] or axisymmetric approximations[13,14] that do not completely represent the three-dimensional geometry or actual loading conditions associated with dental structures. In studies that incorporated three-dimensional representations of teeth, either the geometry or the material's properties were simplified. In some cases, parts of the dental structure such as the pulp, cementum, PDL, or the alveolar bone were disregarded altogether.[15] In addition, the interfacial interactions between the root and its surrounding periodontium have rarely been addressed. Because the PDL is believed to act as a viscoelastic, shock-absorbing, load-transfer medium between the tooth and the alveolar bone,[16] the interfacial load-transfer mechanism of the PDL and its surrounding tooth and alveolar bone should be taken into account when modeling the PDL. We have taken these factors into consideration when constructing our mathematical models.

Ross[7] and Walker[9] conducted experiments to examine creep behavior and determined its dependency on time, displacement, and intraperiodontal pressure (IPP). Although they were unable to fully explain the complex mechanisms of the PDL with their data, they suggested that an explanation could be derived via mathematical modeling. Thus, the primary goal of this study was to investigate the PDL creep source using previously reported human and animal tooth behaviors and finite element analysis to validate the data gathered from Walker's and Ross's experiments and to ascertain the mechanical properties of the PDL. A series of models relating the functions and properties of the PDL were proposed to examine the creep behaviors of the PDL, and, ultimately, the most suitable finite element model for simulating PDL behavior was identified.

Materials and methods

Construction of the finite element models

The construction of the finite element models began by designing the geometric mesh of a tooth based on the dimensions of a sample tooth. In this study, a maxillary central incisor was embedded and sectioned into 19 slices in order to construct a three-dimensional finite element model. The three-dimensional finite element model, which was comprised of the maxillary central incisor, pulp chamber, cementum, PDL, cortical bone, and cancellous bone, consisted of 3772 nodes and 3721 eight-node

isoparametric solid elements. The construction of the finite element model begins with the design of a geometric model of the tooth, which was based on the dimensions of a sample tooth and the general morphology of the maxillary central incisors.[6] Since the width of the PDL ranges from 0.15—0.38 mm at different locations along the tooth,[17] a 0.25-mm-thick layer was created to represent the PDL. The alveolar bone was modeled according to the reported size and shape determined in a related study (Fig. 1).[18] Two analytic programs, ABAQUS 6.2.1 (ABAQUS Inc.) and I-DEAS 8.0 (Siemens PLM Software), were used to construct the finite element models.[17] The mechanical properties of the enamel, dentin, pulp chamber, cementum, cortical bone, and cancellous bone, which were based on the results of previous studies, are listed in Table 1. The boundary conditions at the bottom of the alveolar bone are fixed and asymmetrical, as shown in Fig. 2.

Table 1 Material constants of the finite element model (Goel, 1992).

Tissue	Modulus of elasticity (Mpa)	Poisson's ratio
Enamel	84,000	0.31
Dentin	18,600	0.31
Cementum	18,600	0.31
Cortical Bone	13,700	0.3
Trabecular Bone	1370	0.3
Pulp	2	0.45

The constitutive PDL equation

The basic hereditary integral formulation of linear isotropic viscoelasticity, in terms of its deviatoric and dilatational components, is defined as follows:

$$s_{ij}(t)=2\int_{-\infty}^{t} G(t-\tau)\frac{\partial e_{ij}(\tau)}{\partial\tau}d\tau$$
$$\sigma_{ii}(t)=3\int_{-\infty}^{t} K(t-\tau)\frac{\partial \varepsilon_{jj}(\tau)}{\partial\tau}d\tau \quad (1)$$

where e_{ij} and ε_{jj} are the mechanical deviatoric and volumetric strains, respectively, and $G(t)$ and $K(t)$ are the appropriate relaxation functions of the reduced time, τ, that denote differentiation with respect to t.[19] The relaxation functions, $G(t)$ and $K(t)$, can be individually defined in terms of a series of exponents known as the Prony series:

$$G(t)=G_0\left(g_\infty+\sum_{i=1}^{N} g_i e^{-t/\tau_i}\right), \quad (2)$$

$$K(t)=K_0\left(k_\infty+\sum_{i=1}^{N} k_i e^{-\tau/\tau_i}\right), \quad (3)$$

where G_0 and K_0 are the instantaneous shear and bulk moduli, respectively, and g_i and k_i are the relative moduli of i. Note the following:

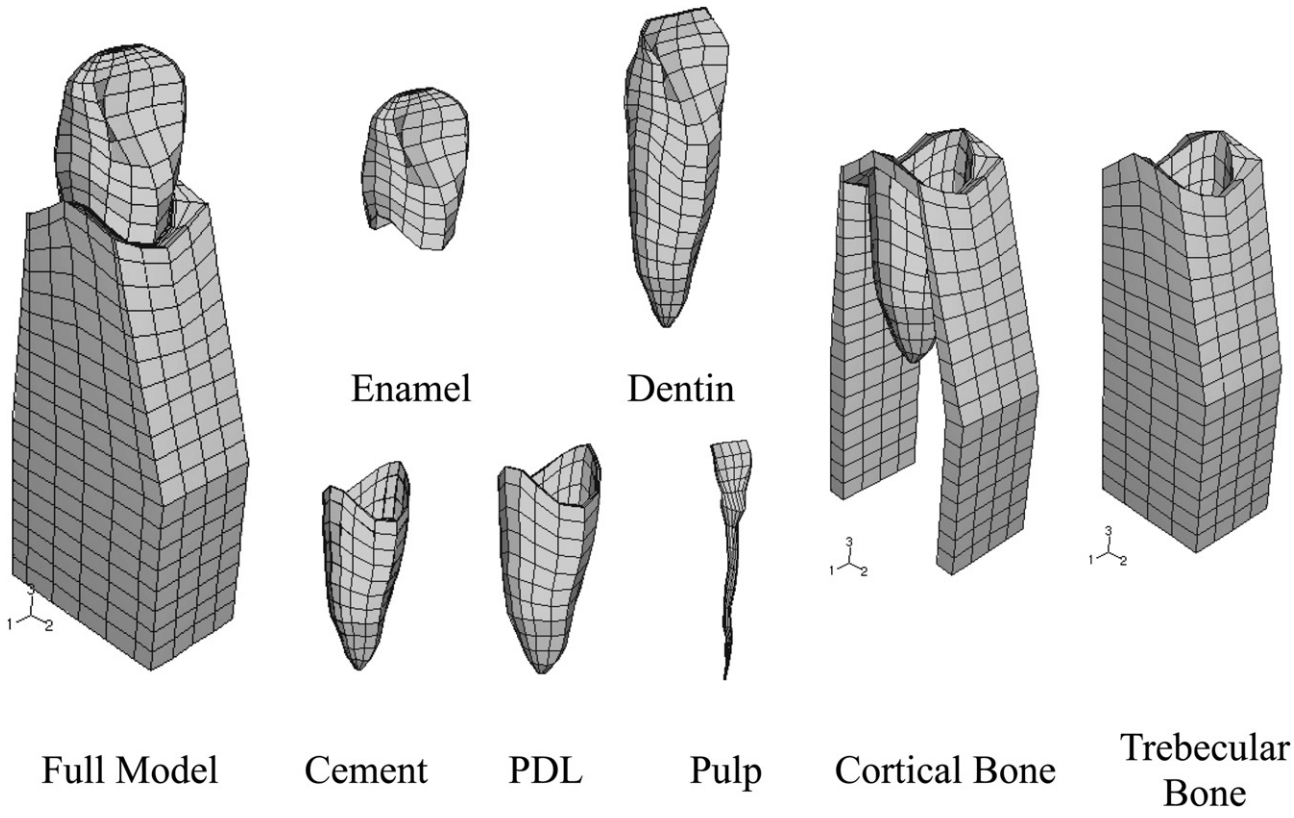

Figure 1 Finite element mesh of the maxillary central incisor.

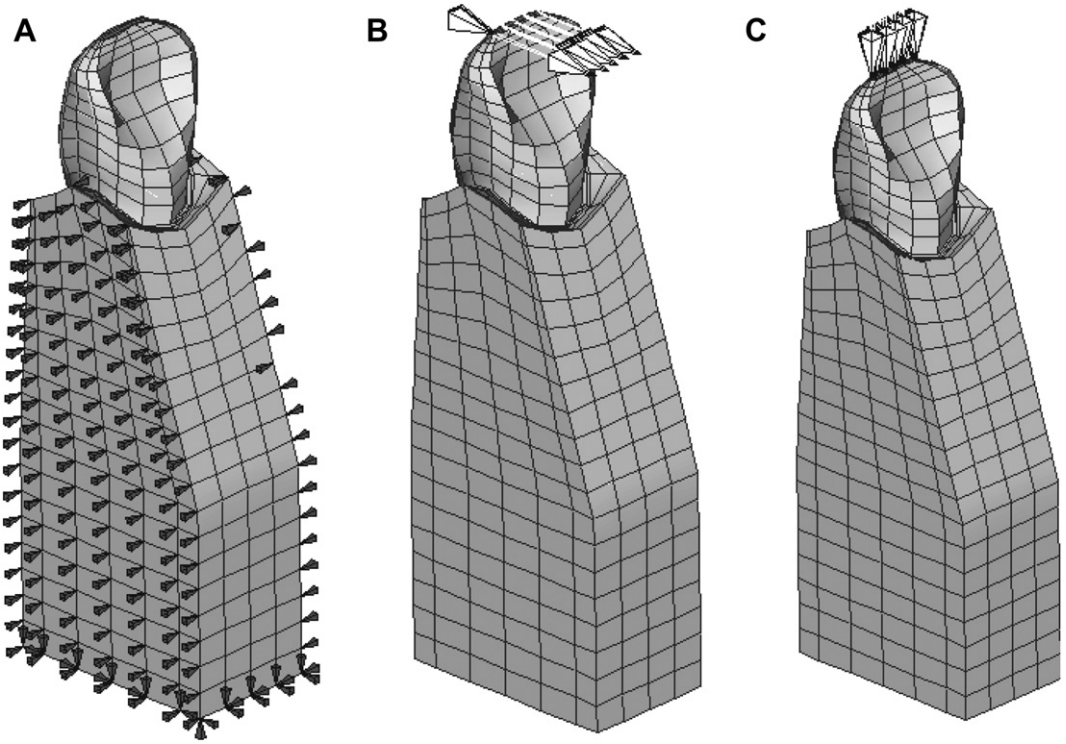

Figure 2 Boundary and loading conditions. (A) Boundary condition. (B) Lateral loading condition. (C) Intrusive loading condition.

$$g_\infty + \sum_{i=1}^{N} g_i e^{-t/\tau_i} = k_\infty + \sum_{i=1}^{N} k_i e^{-\tau/\tau_i} = 1 \tag{4}$$

The volumetric viscoelastic, deviatoric viscoelastic, and tension-compression volumetric viscoelastic models were proposed in order to represent the mechanical properties of the PDL, as shown in Table 2.

In the volumetric viscoelastic model, temporal behavior is derived from the volumetric element of the strain tensor, and the following relaxation functions, *G(t)* and *K(t)*, were chosen to describe the temporal behavior:

$$\begin{aligned} G(t) &= G_0 = \text{constant} \\ K(t) &= K_0\left(k_\infty + k_1 e^{-t/\tau_1} + k_2 e^{-t/\tau_2}\right) \end{aligned} \tag{5}$$

In the deviatoric viscoelastic model, the temporal behavior is derived from the deviatoric portion of the strain tensor, and the following relaxation functions, *G(t)* and *K(t)*, were chosen to describe the temporal behavior:

$$\begin{aligned} G(t) &= G_0\left(g_\infty + g_1 e^{-t/\tau_1} + g_2 e^{-t/\tau_2}\right) \\ K(t) &= K_0 = \text{constant}, \end{aligned} \tag{6}$$

In the tension-compression volumetric viscoelastic model, the temporal behavior is derived from the volumetric portion of the strain tensor, and separate rates of volumetric change were set to differentiate between areas of tension and compression. The relaxation functions, *G(t)* and *K(t)*, were chosen to describe the temporal behavior:

$$\begin{aligned} G(t) &= G_0 = \text{constant} \\ k(t) &= \begin{cases} K_{C0}\left(k_\infty + k_1 e^{-t/\tau_1} + k_2 e^{-t/\tau_2}\right), & \text{for} \varepsilon_{ii} \le 0 \\ K_{T0}\left(k_\infty + k_1 e^{-t/\tau_1} + k_2 e^{-t/\tau_2}\right), & \text{for} \varepsilon_{ii} > 0 \end{cases} \end{aligned} \tag{7}$$

where K_{C0} and K_{T0} are the instantaneous bulk moduli in the areas of compression and tension, respectively. Hence, *G(t)* is constant and *K(t)* is set to be different in areas of tension and compression, respectively.

In the deviatoric viscoelastic model, we assumed that the PDL was incompressible and that the shear-time effect would dominate creep behavior. Meanwhile, the elastic

Table 2 PDL mechanical models and their corresponding creep sources.

Model type	Creep source	Source of material constants	Model assumptions
Volumetric viscoelastic	Free fluid flow	Loading part of the creep experiment by Ross	Volumetric temporal behavior only; linear elastic behavior
Deviatoric viscoelastic	Distortion	Loading part of the creep experiment by Ross	Almost incompressible; deviatoric temporal behavior only; linear elastic behavior
Tension-compression volumetric viscoelastic	Free fluid flow	Entire creep experiment by Ross	Volumetric temporal behavior only; linear elastic behavior

behavior was assumed to be nonlinear because the magnitude of the shear stress may be influenced by the surface of the collagen fibrils and the degree of cross-linking.

Inverse parameter identification process

Because the environmental conditions inside the mouth are too dissimilar from the conditions outside the mouth, ascertaining the true mechanical properties of the PDL via standard means is exceedingly difficult. The inverse identification process, diagrammed in Fig. 3, is a feasible alternative. Based on the viscoelastic constitutive equations, we used the constant loading displacement-time curve from the lateral tooth movement experiment[7] to obtain the mechanical properties of the PDL and, in accordance with that experiment, a 0.05 N lingually directed load was applied, maintained for 2.5 seconds, and then released. The relaxation parameters were defined to correspond to the parameters of the Prony series in ABAQUS, and the optimal parameters were obtained from retrograde calculations using Ross's experimental data. The retrograde calculation method was based on an optimization method that minimizes the square of the tooth displacement error. In general, the objective value equation is written as a function of least squares:

$$\mathrm{Min}Q = \sum_{i=1}^{N} \beta_i \left(D_i^{\mathrm{FEA}} - D_i^{\mathrm{Ross}} \right)^2, \tag{8}$$

where β_i represent the weighted factors necessary to scale the objective value.

To minimize this nonlinear objective function, the complex method, which only uses function values, can be implemented. The complex method[20] is the constrained simplex method that incorporates a direct search algorithm to more efficiently solve the optimization problem associated with the results generated by the ABAQUS software.

In order to study the pressure stress within the PDL during loading, data from Walker's study[7] were used as a reference source for the actual PDL pressure stress responses during loading. In Walker's animal study, pressure recordings in the PDL of canine teeth were divided according to pattern type, and the most common patterns were the positive-peaking (P-response) and sustained pressure (S-response) types. The P-response represents the pressure changes in physiologically normal PDL tissue, whereas the S-response is the product of the traumas sustained by the ligament. In this study, the pressure stresses in the PDL were investigated by modeling a 397 g vertical load to the crown of the tooth in both the deviatoric viscoelastic and tension-compression volumetric viscoelastic models. The pressure stresses from the apex of tooth root to the cementoenamel junction were recorded.

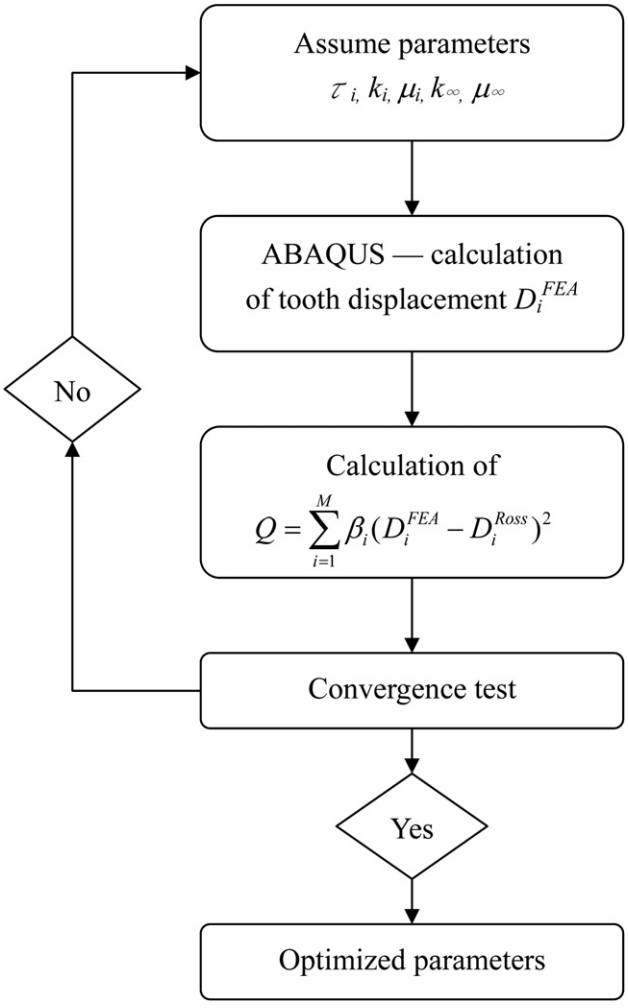

Figure 3 Flow chart of inverse parameters identification procedure.

Finite element stress analysis

Because neither *in vivo* nor *in vitro* studies are capable of determining the internal mechanics of the PDL under loading conditions, finite element models were used in this study to depict the internal stress distribution of the PDL. Using the tension-compression volumetric and deviatoric viscoelastic models, the application of two loading conditions to the crown of the tooth was modeled. First, a 0.05 N lingually directed load was applied, maintained for 2.5 seconds, and then released. Next, a vertical load of the same magnitude was applied and sustained for the same duration. The stress distributions of the dentoalveolar complex during the application of loading and sustained loading were investigated using both models and compared with each other.

Results

Fig. 4 illustrates the creep test data for the volumetric viscoelastic, deviatoric viscoelastic, and tension-compression volumetric viscoelastic models, compared with the data of Ross' Experiment. Most significantly, the volumetric viscoelastic, deviatoric viscoelastic, and tension-compression volumetric viscoelastic models that were implemented in this experiment closely simulated the results from Ross's experiment when loading was applied to the tooth and corresponding PDL. This result indicates that the hereditary integral formulation model for linear isotropic viscoelasticity is capable of approximating the behavior of the PDL

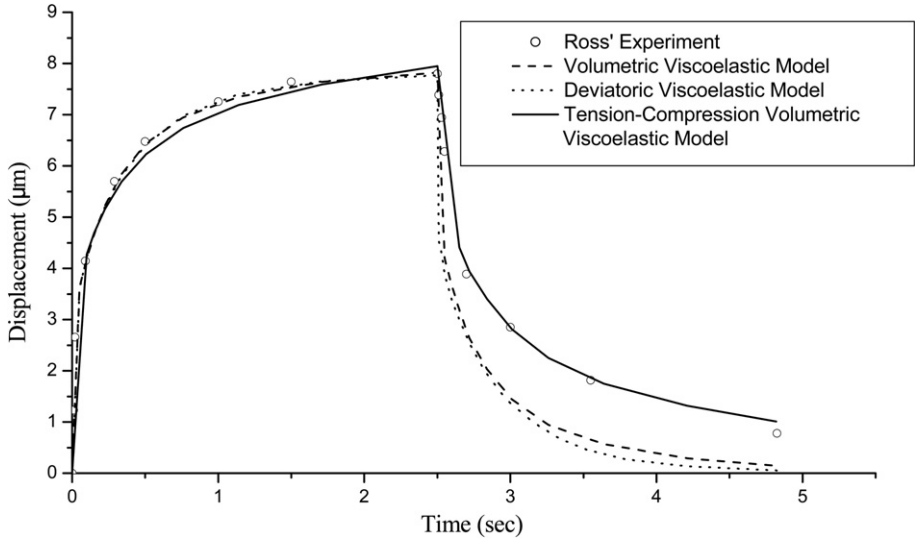

Figure 4 Typical curves of creep test data for the volumetric viscoelastic, deviatoric viscoelastic, and tension-compression volumetric viscoelastic models, compared with the data of Ross' Experiment.

when subjected to loading forces. The viscoelastic properties of the PDL, represented as an elastic modulus and Prony constants in Table 3, were obtained via an inverse parameter identification process. The relaxation functions can be expressed as follows:

1. Volumetric viscoelasticity

$$\begin{aligned} G(t) &= G_0 = 0.0634 \\ K(t) &= 0.076 + 0.454e^{-t/0.0873} + 0.0833e^{-t/0.694} \end{aligned} \quad (9)$$

2. Deviatoric viscoelasticity

$$\begin{aligned} G(t) &= 0.00376 + 0.0391e^{-t/0.0209} + 0.0117e^{-t/0.457} \\ K(t) &= K_0 = 0.89062 \end{aligned} \quad (10)$$

3. Tension-compression volumetric viscoelasticity

$$\begin{aligned} &\text{Tensile area :} \\ &G(t) = G_0 = 0.0133 \\ &K(t) = 0.1032 + 0.4368e^{-t/0.11} + 0.06e^{-t/1.48} \\ &\text{Compressive area :} \\ &G(t) = G_0 = 0.0133 \\ &K(t) = 0.00167 + 0.00708e^{-t/0.11} + 0.000973e^{-t/1.48} \end{aligned} \quad (11)$$

The volumetric and deviatoric viscoelastic mathematical models were not able to use these same sets of constants to accurately reproduce the empirical data from the unloading phase of Ross's experiment. More precisely, the PDL's rate of recovery during unloading seems to be slower than its rate of compression during loading. Thus, the volumetric viscoelastic model was modified to incorporate tensile and compressive relaxation functions to describe PDL behavior during loading and unloading. The elastic modulus and Prony constants obtained via inverse parameter identification from Ross's data are listed in Table 3. When these constants were used, the tension-compression volumetric viscoelastic model was able to emulate the behavior of the PDL during both loading and unloading, as shown in Fig. 4.

Data on IPP were also collected in this study. Fig. 5(A) shows the IPP observed during loading and unloading for the volumetric viscoelastic model. Before loading, IPP was measured at the initial pressure level. When a loading force was applied to the tooth, the volumetric viscoelastic model indicated that the IPP of the corresponding PDL increased sharply before rapidly subsiding to the initial pressure level. Upon unloading, the PDL experienced a similar but inverse effect to its IPP. The resulting IPP pattern during the loading-unloading process bears a striking resemblance to the waveform of the P-response observed in Walker's study.

Fig. 5(B) shows the IPP pattern observed during loading and unloading of the deviatoric viscoelastic model. In

Table 3(a) Mechanical parameters of the volumetric viscoelastic model and deviatoric viscoelastic models for the loading period.

		Volumetric viscoelastic model			Deviatoric viscoelastic model		
Elastic behavior	K_0	0.613			0.891		
	G_0	0.0634			0.0545		
Temporal behavior	Prony constants	N	1	2	N	1	2
		τ_i	0.0873	0.694	τ_i	0.0209	0.0566
		k_i	0.740	0.136	k_i	0	0
		g_i	0	0	g_i	0.717	0.214

Table 3(b) Mechanical parameters of the tension-compression volumetric viscoelastic model.

		Tension-compression volumetric viscoelastic model	
		Tensile area	Compressive area
Elastic behavior	K_0	0.6	0.00973
	G_0	0.0133	0.0133
Temporal behavior	Prony constants	N	1	2
		τ_i	0.11	1.48
		k_i	0.728	0.10

contrast to the IPP levels obtained by the volumetric model, the IPP pattern observed in the deviatoric viscoelastic model resembles the waveform of the S-response observed in Walker's experiment. Although IPP rapidly increased when loading forces were applied, the pressure did not decay as quickly as in the volumetric viscoelastic model. Instead, the IPP remained steady until unloading, during which it immediately decreased to the preloading level.

When lingual loading was applied to the crown of the tooth, the tension-compression volumetric viscoelastic model (Fig. 6) indicated that the pressure stress immediately increased near the cervical area of the PDL. Fig. 6 illustrates that over time the stress dissipated to a slight degree, and the remaining pressure was distributed in a relatively uniform fashion over the entire PDL.

According to the deviatoric viscoelastic model, applying lingual loading to the crown of the tooth also created immediate pressure at the coronal third of the PDL as well at the cervical area, as shown in Fig. 7. During sustained loading, however, the pressure did not dissipate, as suggested by the volumetric viscoelastic model, but rather increased in magnitude as well as coverage area, as illustrated in Fig. 7D. In addition, the pressure due to loading was not distributed along the entire PDL. Instead, the increased stress remained localized near the coronal third of the PDL, as shown in Fig. 7B.

Upon vertical loading in the tension-compression volumetric viscoelastic model, as shown in Fig. 8, the pressure immediately increased in both the root apex and the apical third of the PDL. During sustained vertical loading, the pressure at the apical third of the PDL decreased substantially, and the remaining stress appeared to be uniformly distributed over the entire PDL, as shown in Fig. 8.

The deviatoric viscoelastic model, however, suggests a different scenario for PDL behavior when subjected to vertical loading. Not only did pressure immediately increase at the crown of the tooth, but the entire PDL also experienced an increase in pressure rather than just at the apical third as indicated by the volumetric viscoelastic model. The stress concentration along the PDL, as shown in Fig. 9, increased and reached its maximum intensity along the apical third of the PDL, near the root apex. During sustained loading, the pressure did not dissipate but rather increased in magnitude. Although stress at the coronal third of the PDL decreased slightly, the pressure at the apical third of the PDL increased in both intensity and coverage area, as shown in Fig. 9.

Discussion

The time dependency of the mechanical behavior of the PDL is well known.[21–23] Based on histological findings in the PDL and theories on continuity mechanics, we attributed tooth creep behavior to two possible sources. One source is the volumetric effect, which represents the free fluid in the PDL that flows in the space between the PDL and the alveolar bone; the other source is the deviatoric effect, which corresponds to changes in the shape of the PDL material that occur due to loading effects over time. To study these two sources of tooth creep behavior, we initially constructed two models: the volumetric viscoelastic model and the deviatoric viscoelastic model. By implementing Prony constants and using the results from Ross's lateral tooth movement experiment as a reference, the creep behavior of the PDL was modeled. Both the

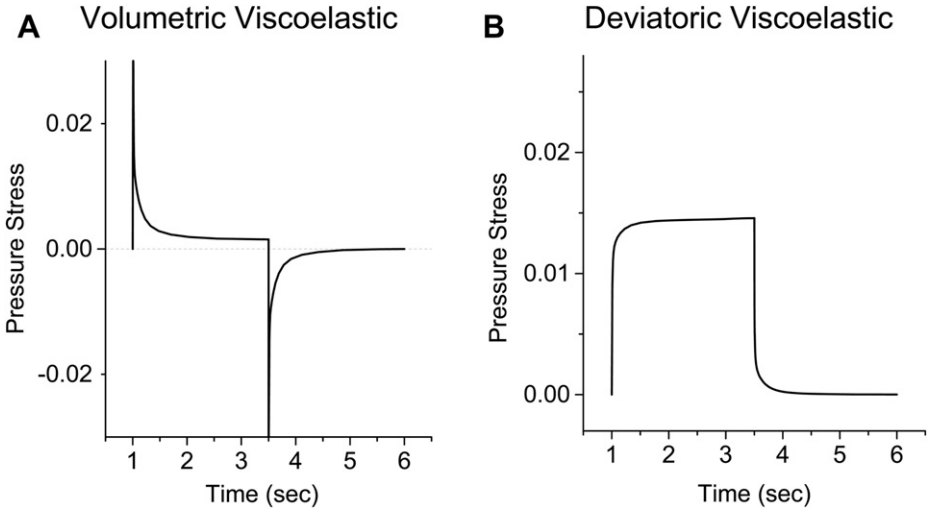

Figure 5 Typical PDL pressure stress in the middle of the root for (A) the tension-compression volumetric viscoelastic model and (B) the deviatoric viscoelastic model.

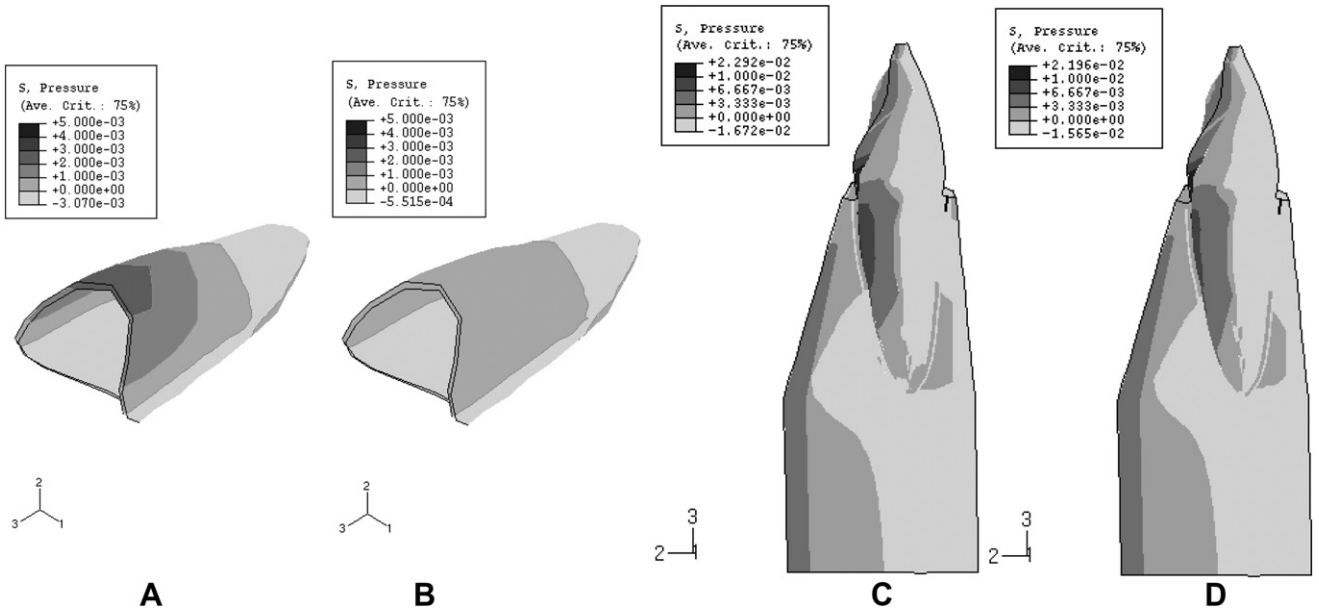

Figure 6 Pressure stress distribution pattern under lateral loading of the tension-compression volumetric viscoelastic model. (A) Pressure stress at t = 0.01 seconds in the PDL. (B) Pressure stress at t = 2.5 seconds in PDL. (C) Pressure stress at t = 0.01 seconds in the labial-lingual direction. (D) The pressure stress at t = 2.5 seconds in the labial-lingual direction.

volumetric viscoelastic and deviatoric viscoelastic models were used to simulate tooth creep behavior, and the corresponding mechanical constants were obtained via retrograde calculation, as shown in Table 3.

A slight discrepancy was found between the displacement-time relationship observed in Ross's experiment and the same relationship that was predicted by both the volumetric viscoelastic and deviatoric viscoelastic models.[7] Although both models were able to approximate the viscoelastic behavior of the PDL during loading with a good degree of accuracy, neither model was able to accurately predict the displacement-time relationship during unloading. We surmise that this discrepancy can be attributed to our assumption that PDL behavior is consistent throughout the entire PDL during both loading and unloading. In fact, the PDL experiences both tension and compression during loading as well as unloading, and in areas of tension fluid enters the PDL while fluid is leaving the PDL in areas of

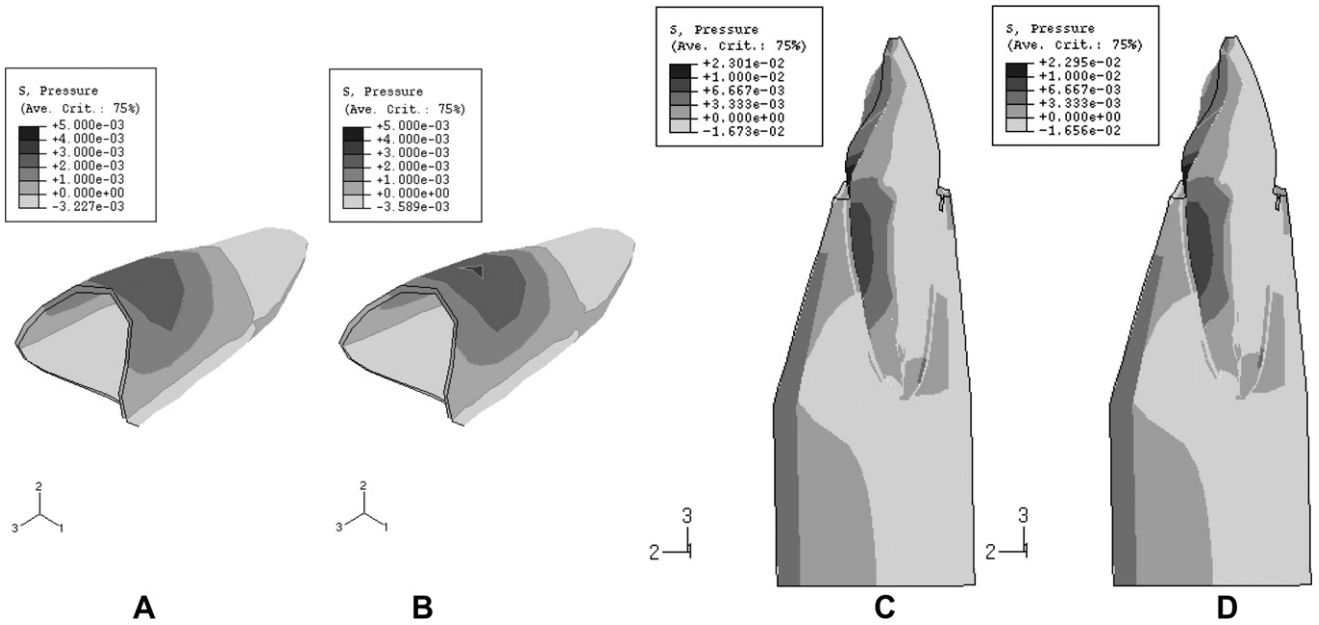

Figure 7 Pressure stress distribution pattern under lateral loading of the deviatoric viscoelastic model. (A) Pressure stress at t = 0.01 seconds in the PDL. (B) Pressure stress at t = 2.5 seconds in the PDL. (C) The pressure stress at t = 0.01 seconds in labial-lingual direction. (D) Pressure stress at t = 2.5 seconds in the labial-lingual direction.

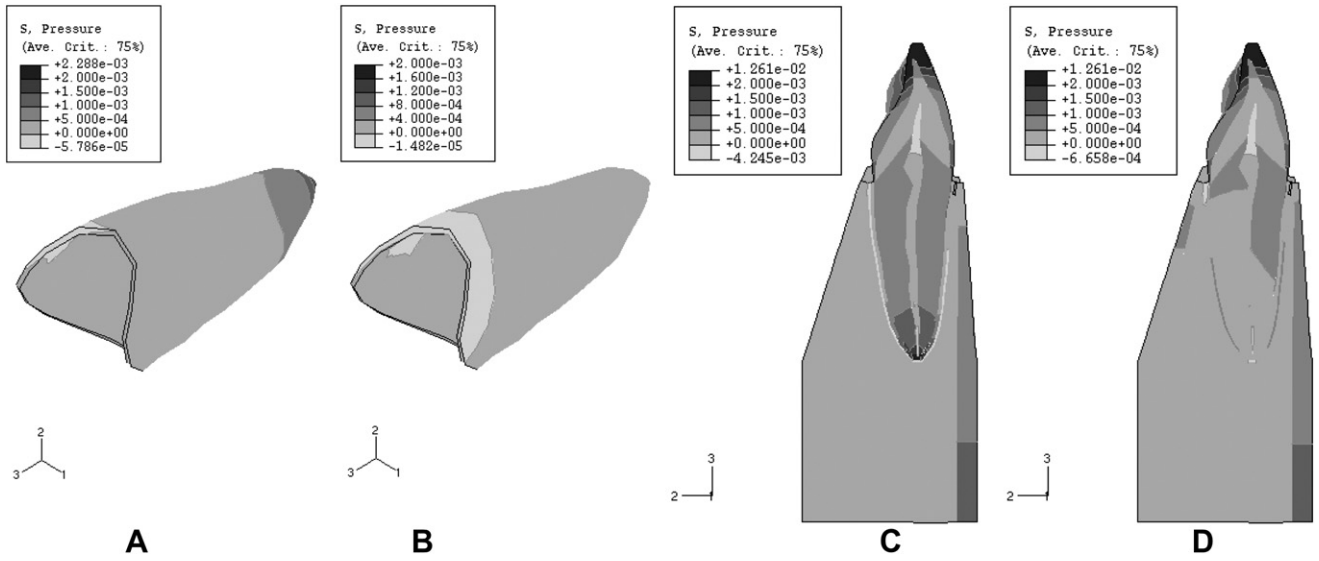

Figure 8 Pressure stress distribution pattern under intrusive loading of the tension-compression volumetric viscoelastic model. (A) Pressure stress at t = 0.01 seconds in the PDL. (B) Pressure stress at t = 2.5 seconds in the PDL. (C) Pressure stress at t = 0.01 seconds in the labial-lingual direction. (D) Pressure stress at t = 2.5 seconds in the labial-lingual direction.

compression. In other words, fluid may simultaneously enter and leave the PDL through different areas during both loading and unloading. The tension-compression volumetric viscoelastic model, which was constructed to take the aforementioned point into account, was able to portray the displacement-time relationship during the entire loading-unloading process. Moreover, the data indicated that the fluid flow rate of fluid leaving the PDL is greater than the flow rate of the fluid entering the PDL. The successful approximation achieved by the tension-compression volumetric viscoelastic model, along with this observed flow rate difference, implies that the inflow rate in areas of compression is greater than the outflow rate in areas of tension. Another implication is that during loading, the majority of the areas along the PDL are in compression, while more areas are tense during unloading.

While the volumetric viscoelastic model was modifiable, the deviatoric viscoelastic model could not be adapted to account for the presence of tension and compression in the PDL during both unloading and unloading. The deviatoric viscoelastic model assumes that the PDL is incompressible and that the shear-time effect dominates PDL creep behavior. Thus, no applicable parameters could be added or changed in the deviatoric viscoelastic model by linear means. Although not included in this study, perhaps a nonlinear method could be utilized to

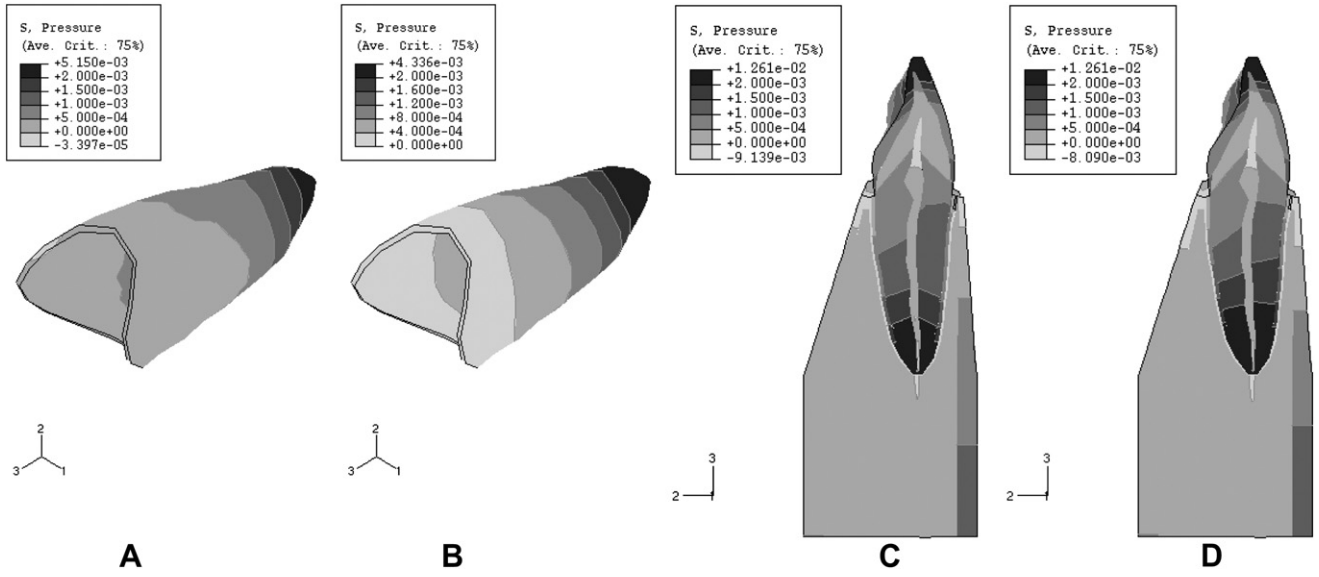

Figure 9 Pressure stress distribution pattern under intrusive loading of the deviatoric viscoelastic model. (A) Pressure stress at t = = 0.01 seconds in the PDL. (B) Pressure stress at t = 2.5 seconds in the PDL. (C) Pressure stress at t = 0.01 seconds in the labial-lingual direction. (D) Pressure stress at t = 2.5 seconds in the labial-lingual direction.

construct an appropriate deviatoric viscoelastic model. While the tension-compression volumetric viscoelastic model incorporates such a parameter, the deviatoric viscoelastic model does not. Consequently, the volumetric effect is most likely the dominant mechanism that affects PDL behavior during loading and unloading.

Based on the pressure stress patterns observed during loading and unloading, we found that the pressure stress patterns in the volumetric-based models (Fig. 4) more closely resemble the fluid pressure changes in the PDL that were observed in Walker's experiment.[9] The pressure stress changes in the PDL of the volumetric-based models match the P-response, and the pressure stress changes in the deviatoric model are similar to the typical S-response. According to Walker's study, the P-response is representative of the behavior of a normal, undamaged PDL, while the S-response represents the behavior of a damaged PDL. Based on the consistency between this study and Walker's experiments with regard to both responses and Walker's reasoning of their significance, several key implications can be inferred. Because the volumetric-based models emphasize the fluidic aspect of the PDL's pressure response system, the observed P-response suggests that an undamaged PDL responds to a loading force by releasing fluid to relieve the added pressure. This rationalization explains why the P-response elicited from the volumetric model demonstrates a rapid increase in pressure followed by a rapid decrease. The fluid release commences after the loading force has been applied. In contrast, the deviatoric model emphasizes the shape-changing aspect of the PDL's pressure response system. The observed S-response suggests that a loading force affects the damaged PDL by compressing its nonfluid parts. This explanation justifies why the pressure level observed in the deviatoric model did not subside like the pressure level in the volumetric-based models. Because a damaged PDL has less fluid to release, its only feasible response to a loading force is to compress its nonfluid components, such as tissue and collagen fibers.

To distinguish between volumetric time effects and deviatoric time effects, we needed to look at the stress patterns and pressure stress changes in a PDL under a constant load. For the tension-compression volumetric viscoelastic model (Figs. 8 and 9), the pressure stress in the PDL under both horizontal and intrusive loading decreased over time. These results concur with the results of both Packman[24] and Walker's[9] studies. In Packman's experiment, circulatory activities were monitored. In areas of the PDL that were compressed, horizontal and axial forces were found to generate a decrease in blood volume. Meanwhile, in areas under tension, the initial increase in blood volume was followed by a decrease as the magnitude of the force rose above the critical level of 90—180 g. The pulse volume, however, increased during both phases.[24] Walker's study recorded fluid pressure changes in the PDL of the canine teeth of dogs during and following the application of loads up to 5.0 N. Moreover, the application of a load caused a sudden pressure increase, which quickly decayed (half-time $<$ 1 second). On the other hand, pressure stresses in the deviatoric viscoelastic model increased over time, which suggests that the major source of viscoelasticity in the PDL comes from the fluid/vascular system of the PDL.[9]

To describe the properties of the PDL, different investigators have suggested various roles for each component of the PDL. Parfitt hypothesized that the displacement of the tooth is largely controlled by fluids in both the vascular and tissue fluid systems.[25] Bien also suggested that the tooth is supported by vascular elements. Bien proposed that the fibers are controlled by the vascular system and that the fibers play only nonessential roles.[5] Packman recorded pastille changes at rest and found that the pastille changes are synchronous with the heartbeat. Packman also reported that loading on a tooth produces a decrease in blood volume in areas under compression, while in areas under tension an initial increase in blood volume was followed by a decrease as the magnitude of force increased. The ground substance of the PDL consists of 70% water, much of which is bound.[24] In Wills's study, the volume of the vascular components of the PDL was found to be approximately 1% of the total volume. However, these systems significantly contributed to tooth support only when forces were $<$ 1.0 N. They also showed that the fluid systems take the responsibility of 30% of the tooth in the tension-compression volumetric viscoelastic model, which is the most appropriate interpretation of normal PDL behavior under loading conditions, and that the deviatoric viscoelastic model is a good representation of how a damaged PDL behaves under loading conditions.[26]

Essentially, this study demonstrates that because it is difficult to ascertain the *in vivo* stress distribution through laboratory experimentation, the method used in this study provides an opportunity to observe stress distributions throughout the tooth and its surrounding tissues. The effects of the distribution of tooth stress on the assumptions of various properties of the periodontium will be addressed in a subsequent study. Further experimental work is required to verify the validity of the assumptions used for model derivation as well as the numerical values of the PDL's material constants. We believe that the biomechanical properties of the PDL that were established via retrograde calculation in this study can lead to the construction of more accurate extra-oral models and the comprehensive understanding of the biomechanical behavior of the PDL.

Acknowledgments

The authors gratefully acknowledge the financial support provided by National Taiwan University Hospital and China Medical University (97F008-107&98F008-211).

In addition, Shao-Huan Tsao, who recently died of leukemia, was one of the authors of this paper. Many of the creative ideas in this paper were inspired and completed by him. This paper would not have been possible without his contributions. Our deepest gratitude goes to Shao-Huan Tsao.

References

1. Nanci A, Ten Cate AR. *Development of tooth and its supporting tissue in Ten Cate's oral histology: development, structure, and function*. 7th ed. New York: Mosby Inc; 2008. p.79—108.

2. Bergomi M, Cugnoni J, Botsis J. The role of the fluid phase in the viscous response of bovine periodontal ligament. *Journal of Biomechanics* 2010;**43**:1146—52.
3. Slomka N, Vardimon AD, Gefen A, Pilo R, Bourauel C, Brosh T, et al. Time-related PDL: viscoelastic response during initial orthodontic tooth movement of a tooth with functioning interproximal contact—a mathematical model. *Journal of Biomechanics* 2008;**41**:1871—7.
4. Berkovitz BKB. The structure of the periodontal ligament: an update. *European J of Orthodontics* 1990;**12**:51—76.
5. Bien SM. Fluid dynamic mechanisms which regulate tooth movement. *Advances in Oral Biology* 1966;**5**:173—201.
6. Picton DCA, Wills DJ. Viscoelastic properties of the periodontal ligament and mucous membrane. *Journal of Prosthetic Dentistry* 1978;**40**:236—72.
7. Ross GG, Lear CS, Decos R. Modeling the lateral movements of teeth. *J Biomechanics* 1976;**9**:723—34.
8. Noriaki Y, Yoshiyuki K, Kazuhide K, Yoshiaki Y, Toshima Y. A new method for qualitative and quantitative evaluation of tooth displacement under the application of orthodontic forces using magnetic sensors. *Medical Engineering and Physics* 2000;**22**: 293—300.
9. Walker TW, Ng GC, Burke PS. Fluid pressures in the periodontal ligament of the mandibular canine tooth in dogs. *Archs Oral Biol* 1978;**23**:753—65.
10. Brekelmans WA, Poort HW, Slooff TJ. A new method to analyse the mechanical behaviour of skeletal parts. *Acta Orthop Scand* 1972;**43**:301—17.
11. Morin DL, Douglas WH, Gross M, DeLong R. Biophysical stress analysis of restored teeth: experimental strain measurement. *Dent Mater* 1988;**4**:41—8.
12. Kampsopra K, Papavasiliou G, Bayne SC, Felton DA. Finite element analysis estimates of cement microfracture under full coverage crowns. *J Prosthet Dent* 1994;**71**:435—41.
13. Rieger MR, Fareed K, Adams WK, Tanquist RA. Bone stress distribution for three endosseous implants. *J Prosthet Dent* 1989;**61**:223—8.
14. Rieger MR, Adams WK, Kinzel GL, Brose MO. Finite element analysis of bone-adapted and bone-bonded endosseous implants. *J Prosthet Dent* 1989;**62**:436—40.
15. Yamna SD, Alacam T, Taman Y. Analysis of stress distribution in a maxillary central incisor subjected to various post and core application. *J Endod* 1998;**24**:107—11.
16. Howard PS, Kucich U, Taliwal R, Korostoff JM. Mechanical forces alter extracellular matrix synthesis by human periodontal ligament fibroblasts. *J Periodontal Res* 1998;**33**:500—8.
17. Götze W. About altersonsveranderungen periodontal. *Dtsch In dentistry AZ* 1965;**15**:465.
18. Tanne K, Yoshida S, Kawata T, Sasaki A, Knox J, Jones ML. An evaluation of the biomechanical response of the tooth and periodontium to orthodontic forces in adolescent and adult subjects. *British Journal of Orthodontics* 1998;**25**:109—15.
19. Hibbit, Karlsson and Sorensen. *ABAQUS Theory Manual. Version 6.2*. USA: ABAQUS Inc.; 2001.
20. Box MJ. A new method of constrained optimization and a comparison with other methods. *The Comp Journal* 1965;**8**: 42—52.
21. Boyle PE. Tooth suspension: a comparative study of the paradental tissues of man and of the guinea pig. *J Dent Res* 1938;**17**:37—46.
22. Picton DCA. The periodontal enigma: eruption versus tooth support. *European Journal of Orthodontics* 1989;**11**:430—9.
23. Picton DCA. Tooth mobility—an update. *European Journal of Orthodontics* 1990;**12**:109—15.
24. Packman H, Shoher I, Stein RS. Vascular responses in the human periodontal ligament and alveolar bone detected by photoelectric plethysmography. *J Periodont* 1977;**52**:903—10.
25. Parfitt GJ. Measurement of the physiological mobility of individual teeth in an axial direction. *J Dent Res* 1960;**39**: 608—18.
26. Bergom M, Cugnoni J, Galli M, Botsis J, Belser UC, Wiskott HW. Hydro-mechanical coupling in the periodontal ligament: a porohyperelastic finite element model. *Journal of Biomechanics* 2011;**4**:34—8.